This ESI for *J. Mater. Chem. A*, 2017, 5, 16994-17000, originally published on 21st July 2017, was updated on 17th December 2018. The order of Fig. S2-S4 has been changed; the fitting curve was added to Fig. S4, an error in the Y-axis label of Fig. S5b has been corrected and the Y-axis scale adjusted.

Supporting Information for:

Engineering Tin Phosphides@Carbon Yolk-Shell Nanocube Structures as a Highly Stable Anode Material for Sodium-Ion Batteries

Lianbo Ma,[†‡]* Pengjie Yan,[‡] Shikui Wu,[‡ǁ] Guoyin Zhu,[†]* Yalong Shen, [‡⊥]*

[†] Key Laboratory of Mesoscopic Chemistry of MOE, School of Chemistry and Chemical Engineering, Nanjing University, Nanjing, 210093, China.

E-mail: mlb8976@126.com (L. Ma); zhuguoyin2008@126.com (G. Zhu)

[‡] School of Chemistry and Chemical Engineering, Jiangsu University, Zhenjiang 212013, PR China.

[ǁ] College of Pharmacy, Inner Mongolia Medical University, Hohhot 010059, PR China.

[⊥] MIIT Key Laboratory of Advanced Display Materials and Devices, Institute of Optoelectronics & Nanomaterials, College of Materials Science and Engineering, Nanjing University of Science and Technology, Nanjing, Jiangsu, 210094, China.

shenyalong@njust.edu.cn (Y. Shen)

Figure S1-S8

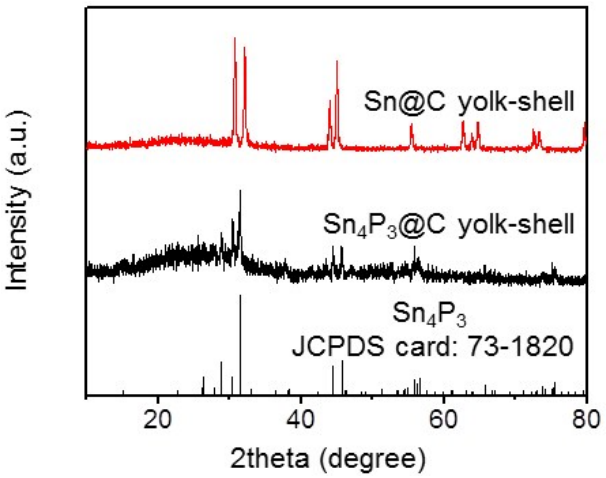

Fig. S1. X-ray diffraction (XRD) patterns of Sn@C and Sn_4P_3@C yolk-shell nanocubes. The XRD pattern of Sn_4P_3@C yolk-shell nanocubes is in good agreement with the standard JCPDS card (No. 73-1820).

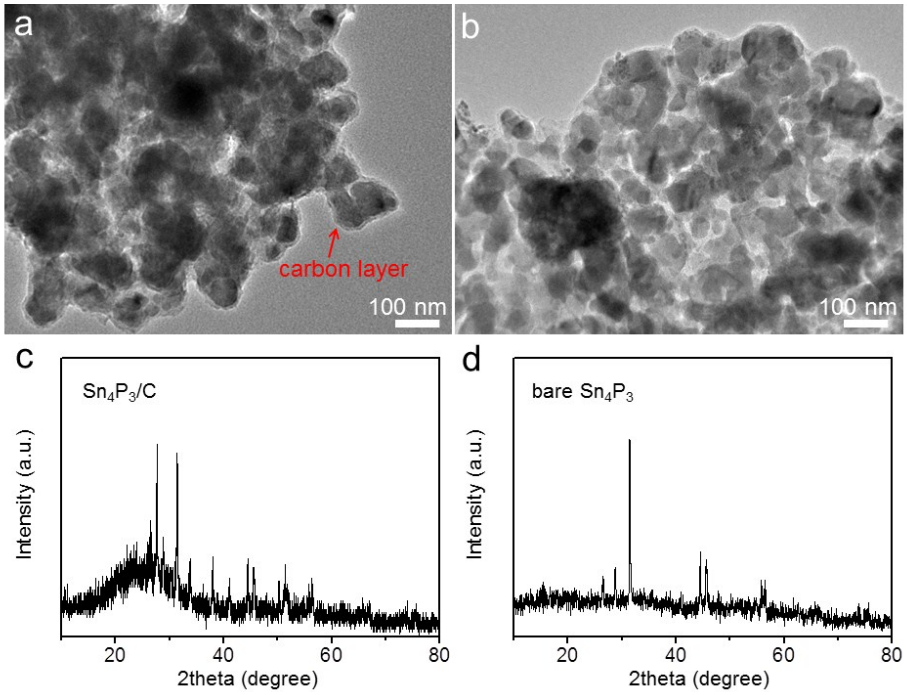

Fig. S2. Morphology and composition characterizations of Sn_4P_3/C and bare Sn_4P_3 as the control samples. (a) TEM image and (c) XRD pattern of Sn_4P_3/C material. (b) TEM image and (d) XRD pattern of bare Sn_4P_3.

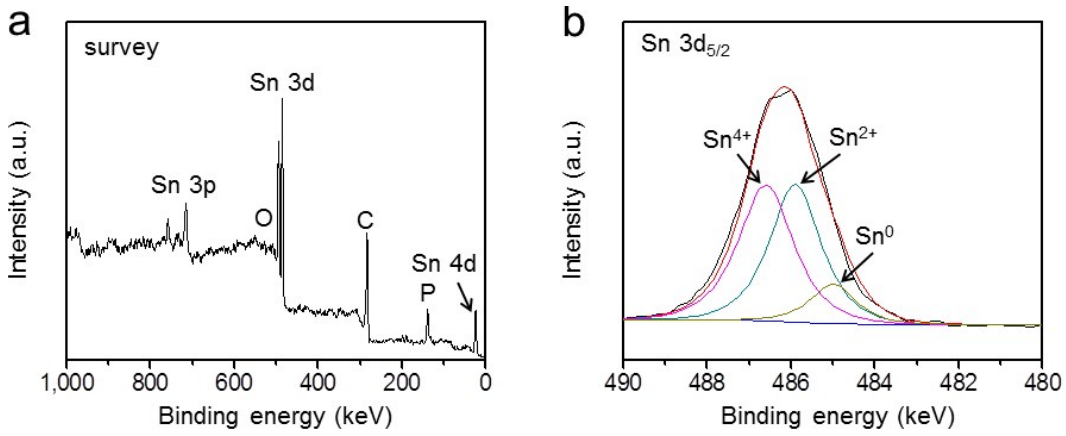

Fig. S3. X-ray photoelectron spectra (XPS) result of Sn_4P_3@C yolk-shell nanocubes. (a) Survey XPS of Sn_4P_3@C yolk-shell nanocubes and (b) the XPS result at Sn $3d_{5/2}$ region. The survey XPS discloses the co-existence of C, Sn and P elements. The Sn $3d_{5/2}$ region suggests the preparation of Sn_4P_3.

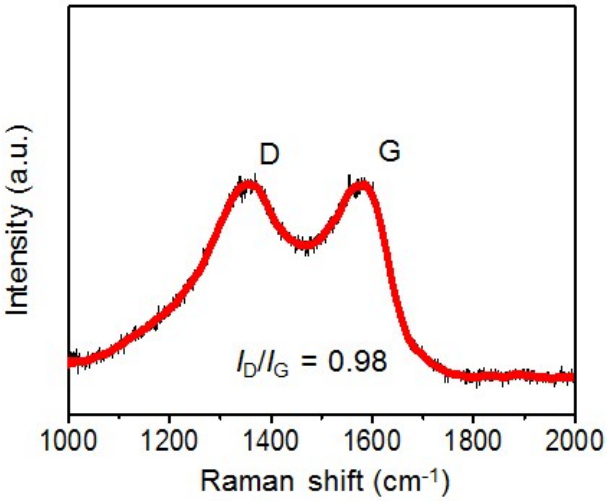

Fig. S4. Raman spectrum of the Sn_4P_3@C yolk-shell nanocubes, revealing the existence of carbon material with moderate graphitic degree.

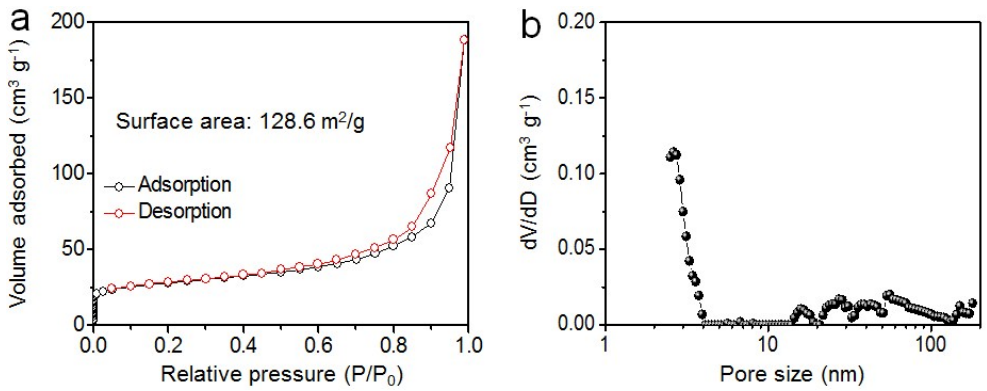

Fig. S5. Surface area and pore size characteristics of Sn_4P_3@C yolk-shell nanocubes. (a) N_2 adsorption-desorption isotherm and (b) pore size distribution of Sn_4P_3@C yolk-shell nanocubes.

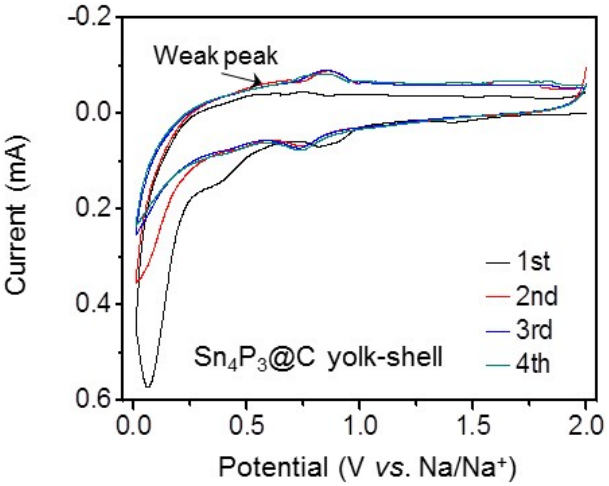

Fig. S6. CV curves of Sn_4P_3@C yolk-shell nanocubes at the scan rate of 0.2 mV s^{-1} within the potential range of 0.01–2.0 V *vs*. Na/Na^+.

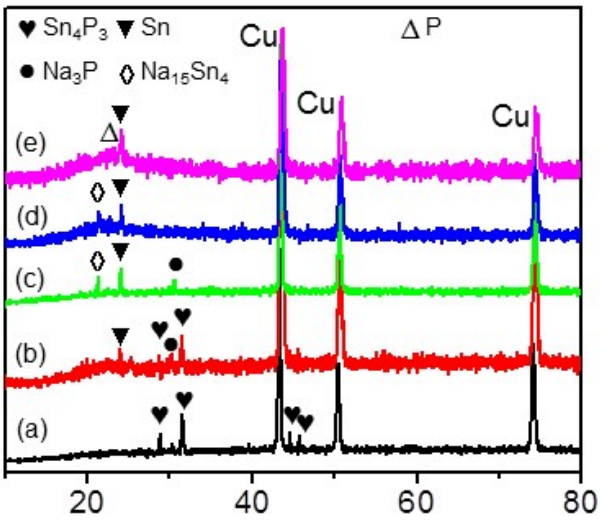

Fig. S7. *Ex-situ* XRD patterns of the Sn_4P_3@C yolk-shell nanocube electrodes at different charge/discharge states: (a) fresh electrode, (b) after first discharge to 0.5 V, (c) after first discharge to 0.01 V, (d) after first charge to 0.5 V, and (e) after first full charge to 2.0 V.

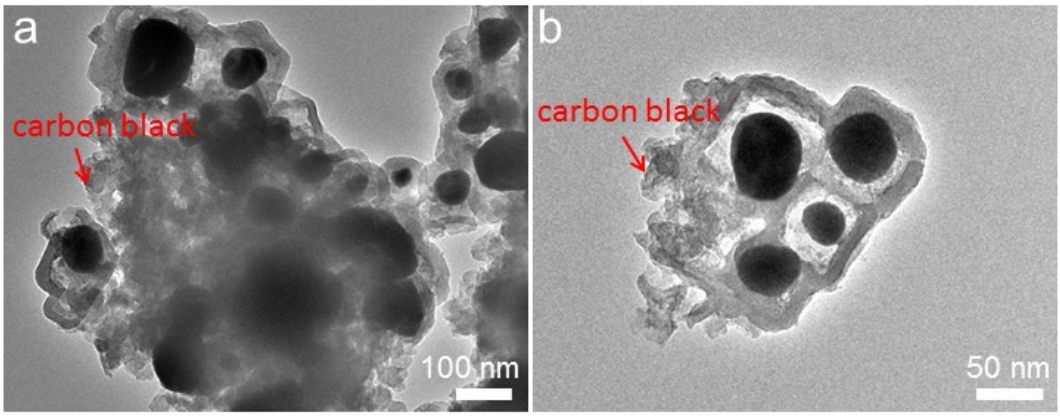

Fig. S8. Morphology of Sn_4P_3@C yolk-shell nanocubes after the electrochemical tests. (a,b) TEM images of Sn_4P_3@C yolk-shell nanocubes after cycling at 2.0 A g^{-1}, showing that the Sn_4P_3 particles were thoroughly encapsulated into the carbon nanocubes, indicating the highly structural integrity.